Low-Frequency Noise Performance of Microstrip-Coupled Lumped-Element Aluminum KIDs using Hydrogenated Amorphous Silicon Parallel-Plate Capacitors for NEW-MUSIC

Simon Hempel-Costello*, Andrew D. Beyer[†], Dan Cunnane [†], Peter K. Day[†], Fabien Defrance[†], Cliff Frez [†], Adriana Gavidia*, Sunil R. Golwala*, Junhan Kim [‡], Jean-Marc Martin*, Yann Sadou*, Jack Sayers*, Shibo Shu[§], Shiling Yu*¶

*Division of Physics, Mathematics, and Astronomy, California Institute of Technology, Pasadena, CA, USA, 91125

[†]Jet Propulsion Laboratory, California Institute of Technology, Pasadena, CA, USA, 91109 [‡] Korea Advanced Institute of Science and Technology, Daejeon, Korea, 34141 [§]Institute of High Energy Physics, Chinese Academy of Sciences, Beijing, China, 100049

National Astronomical Observatories of China, Beijing, China, 100101 University of the Chinese Academy of Sciences, Beijing, China, 101408

Abstract—We present measurements of the low-frequency noise of microstrip-coupled, lumped-element aluminum kinetic inductance detectors that use hydrogenated amorphous silicon parallel-plate capacitors (Al/a-Si:H MS-PPC-LEKIDs), which are under development for the Next-generation Extended Wavelength MUltiband Submillimeter Inductance Camera (NEW-MUSIC). We show that, under dark conditions, these devices are generation recombination (GR) noise dominated down to 0.1 Hz and, under optical load, they are likely dominated by GR and photon noise down to tenths of a Hz and possibly lower, both in spite of the use of a-Si:H PPCs. Our measurements set limits on the lowfrequency two-level-system (TLS) noise of the a-Si:H material that are consistent with higher frequency measurements in the 0.1-10 kHz regime. These results establish that our MS-PPC-LEKID design for NEW-MUSIC will be photon-noise-limited under a range of observing conditions and, more generally, that a-Si:H PPC-KIDs are a viable new detector technology for even low modulation-rate applications such as astronomy.

Index Terms—kinetic inductance detectors (KIDs), superconducting detectors, two-level-system (TLS) noise, millimeter astronomy, submillimeter astronomy

I. INTRODUCTION

THE Next-generation Extended Wavelength MUltiband Submillimeter Inductance Camera (NEW-MUSIC [1]) is an imaging polarimeter with six co-pointed spectral bands spanning 80–420 GHz under development for the Leighton Chajnantor Telescope (LCT). This set of bands will provide access to a a wide range of scientific targets, including: high-frequency synchrotron radiation from a variety of transient and time-domain astronomical sources such as active galactic nuclei and supernovae, gamma-ray bursts, and tidal disruption events expanding in a dense circumstellar medium; diffuse gas in galaxy clusters and the circumgalactic medium via the Sunyaev–Zeldovich effect; dusty, polarized sources in the Milky Way and nearby galaxies; and dusty, star-forming galaxies.

To observe simultaneously across such a large bandwidth over a compact field-of-view, NEW-MUSIC employs frequency-selective hierarchical summing of superconducting phased-array slot-dipole antennas [1], [4], [5], which enables the pixel size to scale with wavelength across 80-420 GHz. These antennas output light onto the superconducting microstripline, necessitating a microstripline-coupled detector. Simultaneously, the detectors must be compact and easily multiplexed because each 6.66 mm side-length pixel feeds 42 individual detectors. Kinetic inductance detectors (KIDs) offer excellent multiplexability, but conventional KID designs using interdigitated capacitors (IDCs) are not sufficiently compact, are not easily microstripline-coupled, and can suffer from direct absorption of light in the inductor and/or the IDC.

To address this need, we have been developing Al/a-Si:H microstripline-coupled, parallel-plate capacitor, lumped-element KIDs (MS-PPC-LEKIDs) [1]–[4]. In this unique KID architecture, a microstripline capacitively couples millimeter/submillimeter waves to an Al KID inductor that sits above a Nb ground plane, providing shielding against direct absorption. The KID incorporates a parallel-plate capacitor (PPC) that is both compact and has inherently low susceptibility to direct absorption.

This architecture requires a dielectric film that has low THz loss for the microstripline and low GHz loss and noise for incorporation into the KID PPC. [7], [8] have shown that deposited hydrogenated amorphous silicon (a-Si:H) dielectric can provide loss and TLS noise performance for GHz resonators comparable to that of IDCs, but TLS noise measurements to date have only been in the 0.1-10 kHz modulation frequency regime and have been done using Nb superconducting resonators, leaving unproven the performance of a-Si:H PPCs for KID astronomical detectors.

In this paper, we characterize the low-frequency noise performance of Al/a-Si:H MS-PPC-LEKIDs, showing they are generation-recombination- or photon-noise limited under dark

2

and optical operation, respectively, down to 0.1 Hz. These measurements demonstrate this KID architecture is stable down to modulation frequencies relevant for astronomical observations (for example corresponding to 5° on the sky at a scan speed of 0.5° /s) and set limits on the TLS noise of our a-Si:H material to much lower frequency than has been explored before.

II. TWO-TONE NOISE MEASUREMENT SETUP

Motivated by the desire to make measurements well below 1 Hz, we developed a two-tone IQ measurement system, which enables the use of a monitor tone to measure and remove multiplicative low-frequency noise frequently seen in RF amplifiers and readout systems. The setup, shown in Fig. 1, uses IQ mixing of a two-tone baseband signal (provided by an arbitrary waveform generator) with a local oscillator (LO) to produce on- and off-resonance probe tones. The up-mixed tones are applied to the KID, amplified cryogenically and at room temperature, IQ-mixed back to their original generation band, amplified again, anti-alias filtered, and digitized. Final demodulation and analysis are performed numerically. In addition to providing a monitor tone, this setup also circumvents the low-frequency additive noise of the generation-band amplifiers by placing both tones at tens to hundreds of kHz. The system is functionally equivalent to a software-defined-radio system with only two tones and a few hundred kHz baseband bandwidth. It has the advantage that all the components are easily accessible and individually testable.

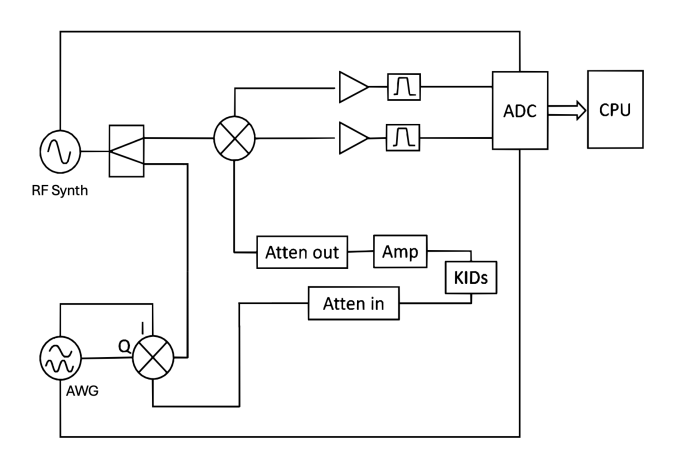


Fig. 1. Two-tone IQ measurement setup. I and Q signals at tens to hundreds of kHz produced by the arbitrary waveform generator (AWG) are up-mixed with a local oscillator (LO) signal from a RF synthesizer. The two-tone signal is sent into the cryostat to probe the KID on and off resonance. The output signal is down-mixed with a copy of the original LO, amplified and anti-alias filtered at baseband, and digitized. Final demodulation of the two tones is done in software. The scheme enables simultaneous acquisition of on- and off-resonance tones to enable removal of correlated multiplicative electronics noise. It also mitigates baseband amplifier additive low-frequency noise.

While we were not able to complete the commissioning of the off-resonance tone for correlated noise removal for this work and thus present only "uncleaned" noise measurements, the setup inherently provides excellent mitigation of additive 1/f noise from the baseband amplifiers for the on-resonance tone alone.

III. TLS Noise Expectation

Our prior measurements of the TLS noise of our a-Si:H PPCs in the 0.1-10 kHz range [7], reproduced here in Fig. 2, enable a prediction for TLS noise in our MS-PPC-LEKIDs at lower frequencies and in the operating conditions used. The scaling relation is

$$S_{TLS} = S_{TLS}^r \left(\frac{T}{246 \text{ mK}}\right)^{-0.8} \frac{A}{A_r} \frac{E}{E_r},$$
 (1)

where A is the capacitor area, E the magnitude of the electric field \vec{E} , and the subscript r denotes reference values from our prior work [7]. That work used broken power law fits to the TLS data,

$$S(f) = \begin{cases} af^{-1} + b, & f \le 100 \text{ Hz,} \\ cf^{-0.5} + d, & f > 100 \text{ Hz,} \end{cases}$$
 (2)

consistent with prior TLS studies that find a transition from $f^{-0.5}$ to f^{-1} scaling near 100 Hz [7].

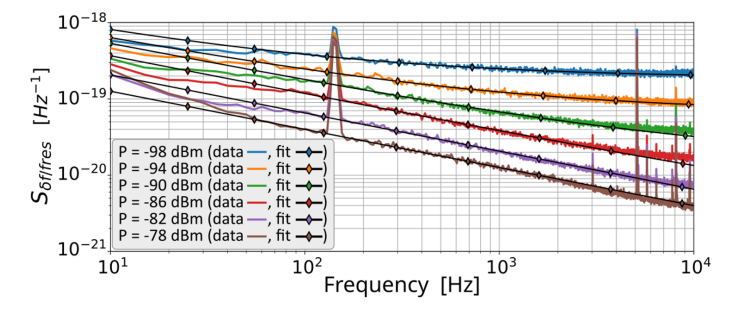


Fig. 2. TLS noise performance of a reference Nb superconducting resonator incorporating a-Si:H dielectric PPCs [7]. Noise PSDs are shown for an 847 MHz resonator. Data were fit with $af^{-0.5} + b$ to capture both TLS and white noise

IV. NOISE MEASUREMENTS AND RESULTS

Noise was measured under both dark and optically loaded conditions. The optical loaded data was taken with $T_{\rm Load} = 77{\rm K} + T_{\rm exc} \approx 180{\rm K}$. Representative noise power spectral densities (PSDs) in fractional frequency units, $S_{\delta f/f}$ are shown in Figs. 3 and 4.

Under dark conditions, the noise PSDs are dominated above ≈ 0.1 Hz by generation-recombination noise. (This point has been verified by checking its temperature dependence [1].) We overlay the expected TLS noise based on scaling using Eq. 1 for the known KID area and for the known feedline readout power and the calculated stored energy in the KID (see, e.g., [8] for the conversion). We plot the scaled TLS noise assuming the given broken power law and assuming extrapolation of the $f^{-0.5}$ power law at all frequencies. The scaling estimates predict TLS noise levels below the noise PSD observed. Thus, while we cannot explicitly check the extrapolation of the TLS noise measurements from [7], we can set upper limits by fitting the $f \leq 100$ Hz form to the observed data, conservatively assuming the rise in noise at low frequency is entirely due to

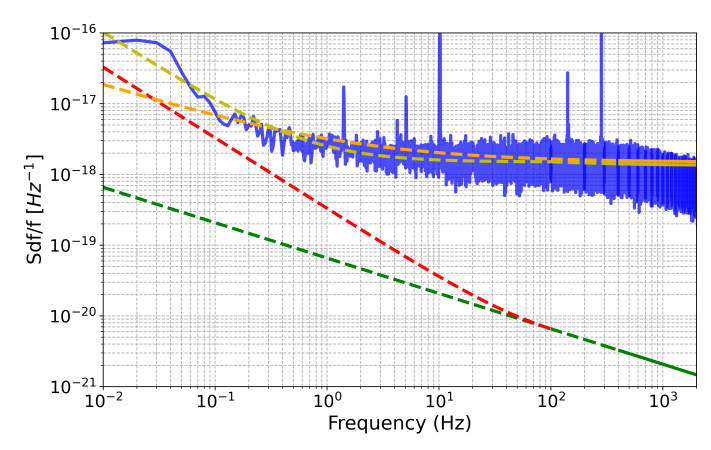


Fig. 3. Dark noise data and TLS noise models. Blue: Noise PSD under dark conditions for an Al MS-PPC-LEKID ($f_r=253.83~\mathrm{MHz}$). Red and green: scaling of TLS noise measured for a-Si:H PPCs in [7] to this resonator's PPC area and electric field for the feedline readout power used. Since [7] only measured noise above 100 Hz, below 100 Hz we show both the Eq. 2 broken power law and a simple f^{-1} extrapolation (red and green, respectively). Mustard and yellow-green: approximate fits of these two models to the measured dark noise PSDs, from which we derive approximate upper limits on TLS noise. It is not certain the low-frequency rise is TLS noise, and there is good reason to think it is not (see text).

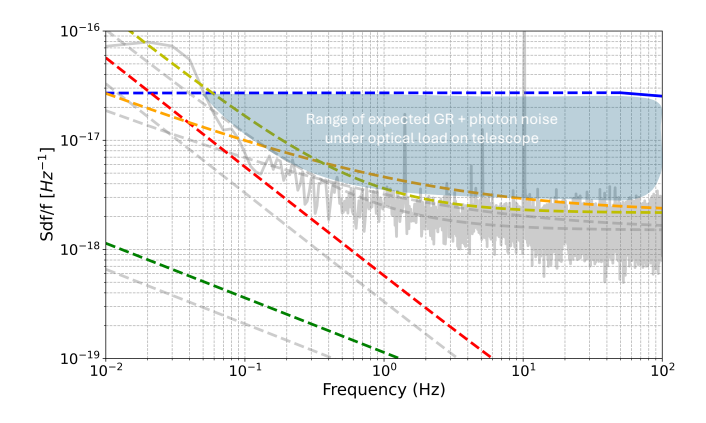


Fig. 4. Noise PSD under optical load, compared to dark noise PSD and TLS noise estimates. Blue solid: GR+photon noise measured above 100 Hz under $T_{Load}=180$ K. Blue dashed: extrapolation of that noise level to low frequency. Grey solid: dark noise PSD. Grey dashed: TLS noise model curves from Fig. 3, unmodified. Colored dashed: the same TLS noise model curves extrapolated to the operating conditions under optical load (i.e., scaling by electric field magnitude): they increase because the stored power decreases. Discussion is provided in the text.

TLS.¹ We thus obtain an approximate upper limit of 3.5 times the broken power-law model and 56 times the extrapolated $f^{-0.5}$ model.

Under optical load, the noise has only been reliably measured above 100 Hz (those measurements, previously reported in [1], did not use the two-tone setup. They showed a dependence on optical load consistent with domination by GR+photon noise [1]. We thus extrapolate this measured noise down to 0.01 Hz in the figure. We overlay the noise PSD

¹We have no definite evidence it is TLS. In fact, the appearance of a similar rise in the dissipation-direction noise PSD (not shown here), which should not be subject to TLS noise, suggests the rise is correlated electronics noise. Future measurements will benefit from removal of correlated noise using the off-resonance tone in the two-tone setup and may set more stringent limits.

from the dark data. Because the optical load was $\approx 180~\rm K$, and we expect the optical load on the sky will be 40–150 K (depending on spectral band) [1], and because the KID responsivity $d(\delta f/f)/dP_{opt}$ decreases with increasing load, the photon noise under on-sky conditions will likely be between the dark GR noise PSD and the optical GR+photon noise PSD. A collusion of the dependence of responsibility and photon noise on loading could possibly cause the photon noise in $S_{\delta f/f}$ to exceed the value measured at $T_{Load}=180~\rm K$; if so, our analysis below is conservative.

Next, we scale both the TLS noise measurements from [7] and the upper limit from the dark data to the optically loaded operating conditions and compare to the extrapolated GR+photon noise. These scalings are the various other colored curves in Fig. 4. We see that even the most conservative case - the broken power law upper limit — implies photon noise dominates down to 0.1 Hz under 180 K optical load. For intervening optical loads, between dark and 180 K, the photon noise will likely lie between the 180 K noise and the dark noise, while the TLS noise will lie between the colored and companion grey curves shown Fig. 4. The crossing point of the photon noise and scaled TLS noise upper limits may thus, conservatively, reach into the tenths of a Hz. The crossing point may in fact be lower if the low-frequency rise seen in the dark data is removable electronics, rather than TLS, noise.¹ If the prediction from from [7] is correct, the crossing point is 0.1-0.2 Hz (broken power law) or lower frequency (f^{-1} power law).

V. CONCLUSION

In this paper, we measured the low-frequency noise of Al/a-Si:H MS-PPC-LEKIDs of the NEW-MUSIC design under dark conditions, observing GR noise down to 0.1 Hz. The upper limits we can set on TLS noise are a factor of 3.5 to 56 above the expectation based on scaling of TLS noise measurements of a-Si:H PPCs in [7] but consistent with those predictions, as there is no evidence the low-frequency noise observed is due to TLS.

We then scaled both our upper limits from the dark data as well as the results of [7] to operating conditions under optical load and compared to GR+photon noise measured at $T_{Load}=180~\rm K$. We conservatively concluded from this comparison that these detectors should be dominated by GR and photon noise down to tenths of a Hz and possibly lower, corresponding to between 1° and 5° on the sky at 0.5° /s scan speed. These results bode well for the use of our Al/a-Si:H MS-PPC-LEKIDs for astronomical observations in NEW-MUSIC, and they more generally validate the utility of a-Si:H PPCs for KIDs.

ACKNOWLEDGMENTS

This work was supported by funding from the National Aeronautics and Space Administration (NASA), the NASA Jet Propulsion Laboratory (JPL), the Department of Energy (DOE), the Wilf Foundation, and by Caltech. A portion of this research was carried out at the Jet Propulsion Laboratory, California Institute of Technology, under a contract

with the National Aeronautics and Space Administration (80NM0018D0004). The authors acknowledge the work of numerous former students and collaborators in the development of the Al/a-Si:H MS-PPC-LEKID architecture.

REFERENCES

- S. R. Golwala et al., "NEW-MUSIC: The Next-generation Extended-Wavelength MUltiband Sub/millimeter Inductance Camera," Proc. SPIE, Aug. 2024, p. 1310202. doi: 10.1117/12.3021175.
- [2] C. Ji et al., "Design of antenna-coupled lumped-element titanium nitride KIDs for long-wavelength multi-band continuum imaging", Proc. SPIE, vol. 9153, p. 915321, Jul. 2014, doi: 10.1117/12.2056777.
 [3] S. Shu et al., "A Multi-chroic Kinetic Inductance Detectors Array Using
- [3] S. Shu et al., "A Multi-chroic Kinetic Inductance Detectors Array Using Hierarchical Phased Array Antenna", J. Low Temp. Phys, vol. 209, p. 330, Nov. 2022, doi: 10.1007/s10909-022-02890-x
- 330, Nov. 2022, doi: 10.1007/s10909-022-02890-x.
 [4] J.-M. Martin et al., "Hierarchical Phased-Array Antennas Coupled to Al KIDs: A Scalable Architecture for Multi-band Millimeter/Submillimeter Focal Planes", J. Low Temp. Phys, vol. 216, p. 104, Jul. 2024, doi: 10.1007/s10909-024-03110-4.
- [5] X. Huang et al., "Design of a Six-band, 2.5-Octave (75–420 GHz) Hierarchically Summed Phased-Array Slot-Dipole Antenna Array for NEW-MUSIC", this volume.
- [6] J. Zmuidzinas, "Superconducting Microresonators: Physics and Applications," Annu. Rev. Condens. Matter Phys., vol. 3, no. 1, pp. 169–214, Mar. 2012, doi: 10.1146/annurev-conmatphys-020911-125022.
- [7] F. Defrance, et al., "Low two-level-system noise in hydrogenated amorphous silicon," Appl. Phys. Lett., vol. 126, p. 122904, Mar. 2025, doi: 10.1063/5.0255172.
- [8] F. Defrance et al., "Characterization of the low electric field and zero-temperature two-level-system loss in hydrogenated amorphous silicon," Phys. Rev. Materials, vol. 8, no. 3, p. 035602, Mar. 2024, doi: 10.1103/PhysRevMaterials.8.035602.